Scaling properties of vortex ring formation at a circular tube opening

Monika Nitsche[a)]

Institute for Mathematics and its Applications, University of Minnesota, 514 Vincent Hall,
206 Church St. SE, Minneapolis, Minnesota 55455

A vortex sheet model is applied to study vortex ring formation at the edge of a circular tube, for accelerating piston velocities $U_p \sim t^m$. We determine properties of the vortex ring as a function of the piston motion and investigate the extent to which similarity theory for planar vortex sheet separation applies. For piston strokes up to half the tube diameter, we find that the ring diameter, core size and circulation are well predicted by the planar similarity theory. The axial ring translation is a superposition of an upstream component predicted by the theory and a downstream component which is linear in the piston stroke. The front of the fluid volume exiting the tube is also linear in the piston stroke and travels with 75% of the piston velocity. The core size decreases and the distribution of fluid near the core becomes more asymmetric as the parameter m increases. © *1996 American Institute of Physics.* [S1070-6631(96)02407-5]

I. INTRODUCTION

A typical experiment of vortex ring formation at a tube opening is shown in Fig. 1(a). It consists of a circular tube immersed in fluid and a piston inside the tube which moves, ejecting fluid from the opening. This causes the boundary layer on the inner tube wall to separate at the edge as an axisymmetric shear layer, which then rolls up and forms a vortex ring. One objective of vortex ring experiments has been to describe the ring properties as a function of the generating conditions (Shariff and Leonard[1]). For the tube geometry, the relevant condition is the piston velocity. In this paper we use a numerical vortex sheet model to investigate the dependence of the ring trajectory, circulation, size and shape on accelerating piston velocities of the form $U_p(t) \sim t^m$.

Theoretical predictions based on similarity theory have been obtained for the planar flow shown in Fig. 1(b). Here, flow around the edge of a semi-infinite flat plate causes the separation and roll-up of a planar shear layer. After an initial time-interval the viscous shear layer thickness is small relative to the size of the roll-up and the separated layer is well approximated by a vortex sheet. The vortex sheet represents the layer by a surface which moves in inviscid flow. There is no length scale in the flow which implies that the vortex sheet separation is self-similar. The scaling behavior of the spiral center, size and circulation can be determined for starting flows that satisfy a power law in time. Pullin[2] discusses the similarity theory for the planar flow and computes the self-similar shape of the roll-up using a numerical method.

The similarity scaling laws depend on the form of the potential flow around the plate. Near the edge, axisymmetric potential flow out of a tube is similar to planar potential flow around a plate. It is therefore plausible to assume that at small times the axisymmetric separation in Fig. 1(a) is approximated by the planar separation in Fig. 1(b). The planar similarity theory can then be used to predict the vortex ring

trajectory, shape and circulation, for the case of power law piston velocity (Saffman[3], Pullin[4]). Didden[5] performed an experiment in which the piston velocity was constant after an initial start-up period. He observed that, while the radial ring coordinate appeared to agree with planar similarity theory, the axial coordinate did not. It has been unclear whether any scaling law does describe the axial ring coordinate[1]. The discrepancy observed by Didden is related to the following difference between the planar and the axisymmetric flow. In the planar case, the self-similar spiral center travels upstream (with negative horizontal velocity) along a straight line [dotted line in Fig. 1(b)] while in the axisymmetric case, the vortex ring travels downstream (with positive axial velocity) along a curved trajectory[5] [dotted curve in Fig. 1(a)]. The axisymmetric flow thus does not resemble the planar self-similar flow and it is not clear *a priori* to what extent the planar similarity theory describes the axisymmetric flow.

Nitsche and Krasny[6] developed an axisymmetric vortex sheet model for vortex ring formation at the edge of a circular tube and simulated the experiment performed by Didden[5]. Comparison with experimental measurements showed that the model accurately recovers the formation process. In this paper we apply the model to simulate vortex ring formation for accelerating piston velocities $U_p \sim t^m$, where we consider $m = 0, 1/2, 1, 2$. The case $m = 0$ corresponds to the case studied by Didden. Unlike a laboratory experiment, the computations do not require a start-up flow and the prescribed piston velocity profile can be satisfied exactly. Here we use the computations to investigate the flow and determine the extent to which it is described by planar similarity theory.

II. SIMILARITY THEORY

The scaling laws governing planar vortex sheet separation at the edge of a flat plate are derived in Pullin[2]. The vortex sheet is embedded in an otherwise potential flow, which Pullin took to grow in time as t^m. To leading order near the edge of the plate, the attached flow has velocity potential

$$\phi(r, \theta) = -i a t^m r^{1/2} \sin(\theta/2). \tag{1}$$

[a)]Telephone: (612) 624-6066; fax: (612) 626-7370; electronic mail: nitsche@ima.umn.edu
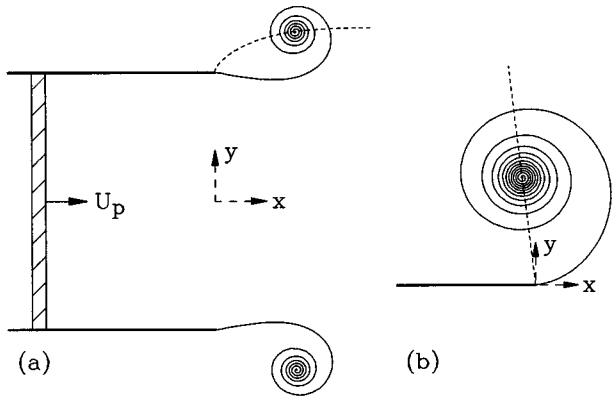
FIG. 1. (a) Axisymmetric vortex ring formation at the edge of a circular tube. (b) Planar vortex sheet separation at the edge of a flat plate.

Here, (r,θ) are polar coordinates centered at the edge and a is a dimensional constant. From dimensional analysis of the governing equations it follows that the center of the separated spiral vortex sheet, $z_c = x_c + i y_c$, and the total shed circulation Γ, satisfy

$$z_c(t) = \omega(m)\left[\frac{3a/4}{m+1}\right]^{2/3} t^{(2/3)(m+1)},$$

$$\Gamma(t) = J(m)\left[\frac{3a^4/4}{m+1}\right]^{1/3} t^{(4/3)(1+m)-1}. \tag{2}$$

The numbers ω, J are nondimensional and depend on m. Under the scaling laws (2), the governing equations reduce to an integro-differential equation independent of time. Pullin solved this equation by approximating the shed vortex sheet by a finite number of outer turns and representing the
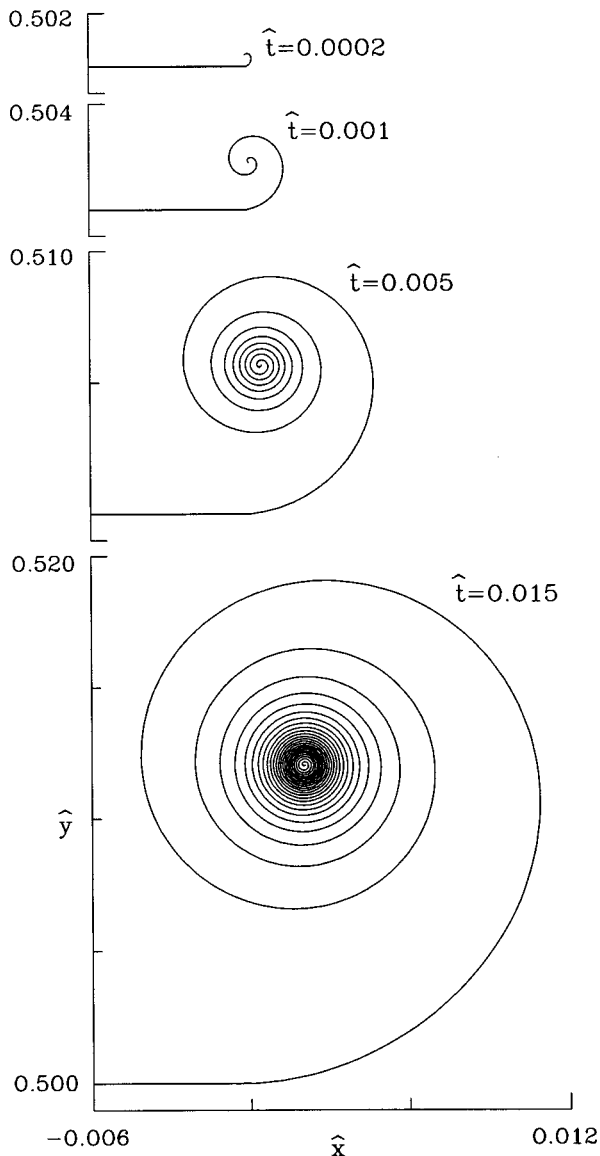

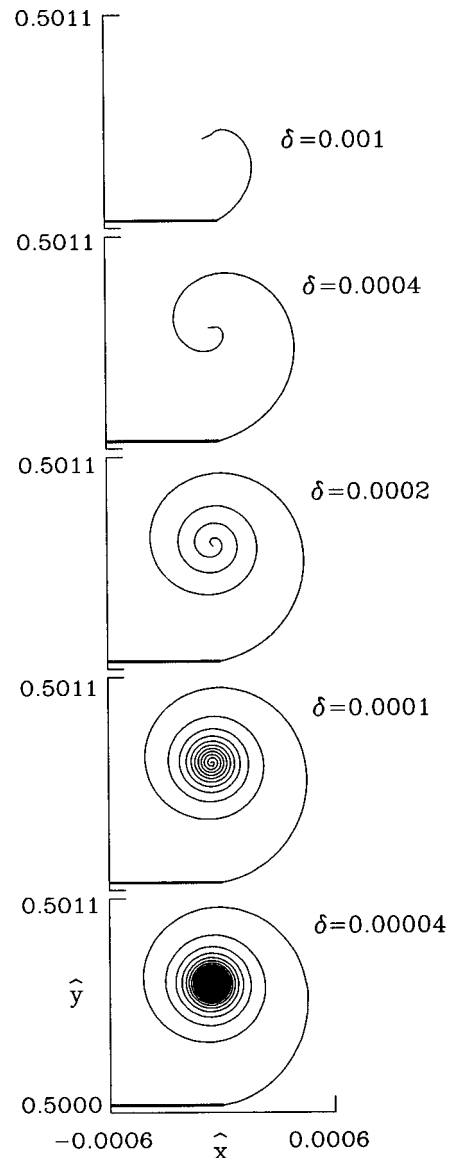FIG. 2. Computed solution at the indicated values of $\hat{t}$, with $\delta = 0.001$ and $m = 0$.

FIG. 3. Computed solution at $\hat{t} = 0.0002$, with the indicated values of δ ($m = 0$).

Phys. Fluids, Vol. 8, No. 7, July 1996

Monika Nitsche   1849

remaining inner spiral core as a point vortex. He recorded the solution for a range of values of m. Krasny[7] solved the time dependent problem using a planar vortex sheet model and found good agreement with Pullin's solution.

Pullin[4] applied the planar similarity theory to axisymmetric flow out of a circular tube. For piston velocities

$$U_p(t) = U_o t^m, \tag{3}$$

the velocity potential near the tube opening has the same form as the planar potential (1). Using the dimensions of the constant a in (1) and a computed estimate for the magnitude of the potential, Pullin found that $a = U_o(D_o/2\pi)^{1/2}$, where D_o is the tube diameter. It is thus expected that the axisymmetric separation approximately satisfies (2) with this value of a.

Following Pullin we introduce nondimensional variables,

$$\hat{t} = \frac{\bar{U}_o t}{D_o}, \quad \hat{\Gamma} = \frac{\Gamma}{\bar{U}_o D_o}, \quad \hat{z}_c = \frac{z_c}{D_o}. \tag{4}$$

Here, $\bar{U}_o$ is the average velocity at time t, $\bar{U}_o = (1/t)\int_o^t U_p(\xi)d\xi$, and $\hat{t}$ equals the nondimensional piston stroke at time t. With this change of variables and the given value of a, (2) reduces to

$$\hat{z}_c = C_{z_c} \hat{t}^{2/3}, \quad \hat{\Gamma} = C_\Gamma \hat{t}^{1/3}, \tag{5}$$

where $C_{z_c} = C_{x_c} + iC_{y_c} = \omega(m)(9/32\pi)^{1/3}$ and $C_\Gamma = J(m) \times (1+m)(3/16\pi^2)^{1/3}$. Throughout the rest of this paper, all variables are nondimensionalized as in (4).

III. NUMERICAL METHOD AND SOLUTION

The axisymmetric vortex sheet model and its numerical implementation are discussed in detail in Nitsche and Krasny[6] and will only be briefly described here. The tube wall and back are modelled by a bound vortex sheet whose strength is such that the induced flow is tangent to the wall and equals the piston velocity in the rear of the tube. The separated shear layer is modelled by a free vortex sheet. Both the bound and the free vortex sheet are discretized by circular vortex filaments. Vortex shedding is simulated by releasing a filament from the edge at each time-step, with velocity equal to the average velocity at the edge and circulation given by Prandtl's slip flow model for separation at a sharp edge[8]. The spiral roll-up of the free vortex sheet is resolved using the vortex blob method, in which a smoothing parameter δ is introduced into the governing equations. The computations are performed with $\delta > 0$ and the vortex sheet is obtained from the limit $\delta \to 0$.

Figures 2 and 3 show the solution computed for impulsively started piston motion, $m = 0$. Each plot shows a section of the tube and a curve connecting the shed vortex filaments. The coordinate system is as indicated in Fig. 1(a). Figure 2 shows the solution computed with a fixed value of δ. The vortex sheet shed from the edge rolls up into a spiral. As time increases, the spiral grows and the number of spiral turns increases. To resolve the roll-up at small times, the flow is computed with smaller values of δ. As an example,
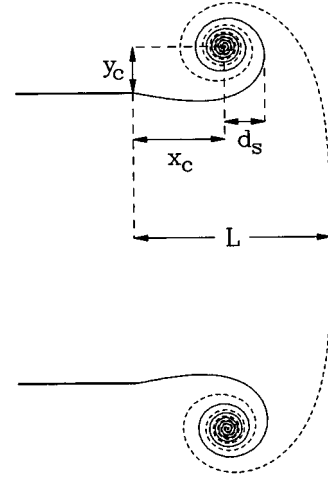

FIG. 4. Sketch showing definitions. x_c, y_c: spiral center coordinates, d_s: spiral half diameter, L: distance travelled by a particle initially on the axis in the tube exit plane.

Fig. 3 shows the solution at $\hat{t} = 0.0002$ computed with a decreasing sequence of δ. We note that δ, which scales as a length, has also been nondimensionalized.

IV. COMPARISON WITH SIMILARITY THEORY

We investigate the behavior of various quantities as a function of the nondimensional piston stroke $\hat{t}$. Figure 4 shows the definition of the vortex center coordinates x_c, y_c, the spiral half diameter d_s, and the distance L travelled by a particle initially on the axis in the tube exit plane. The dashed curve denotes the position of a material curve initially across the tube opening. Together with the free vortex sheet (solid curve), the dashed curve therefore bounds the fluid initially inside the tube from the fluid initially outside the tube. Γ is the total circulation shed from the edge at time t. Figures 5–7 describe the computed behavior of these quantities, for impulsively started piston motion, $m = 0$. The variables y_c, d_s, L and Γ are monotonically increasing in time and are treated first; the axial ring coordinate x_c is treated separately. The shape of the roll-up as a function of m is discussed last.

A. Radial coordinate y_c, spiral diameter d_s, circulation Γ and distance L

Figure 5 shows log-log plots of the computed quantities $\hat{y}_c$, $\hat{d}_s$, $\hat{\Gamma}$ and $\hat{L}$, vs the piston stroke $\hat{t}$. For each quantity, various curves are shown, corresponding to values of $\delta \in [0.00002, 0.02]$. For each value of δ, the curve is not plotted at early times for which no spiral turns have yet formed. The curves converge to an envelope which appears linear for $\hat{t} < 0.5$. Thus, the quantities obey a power law at these times,

$$\hat{q} = C_q \hat{t}^{p_q}. \tag{6}$$

Each subplot also shows a line whose slope closely approximates the one of the envelope. In the cases (a,b,c) the slope of the line is the value predicted by planar similarity theory. Similarity theory does not give a prediction for the quantity
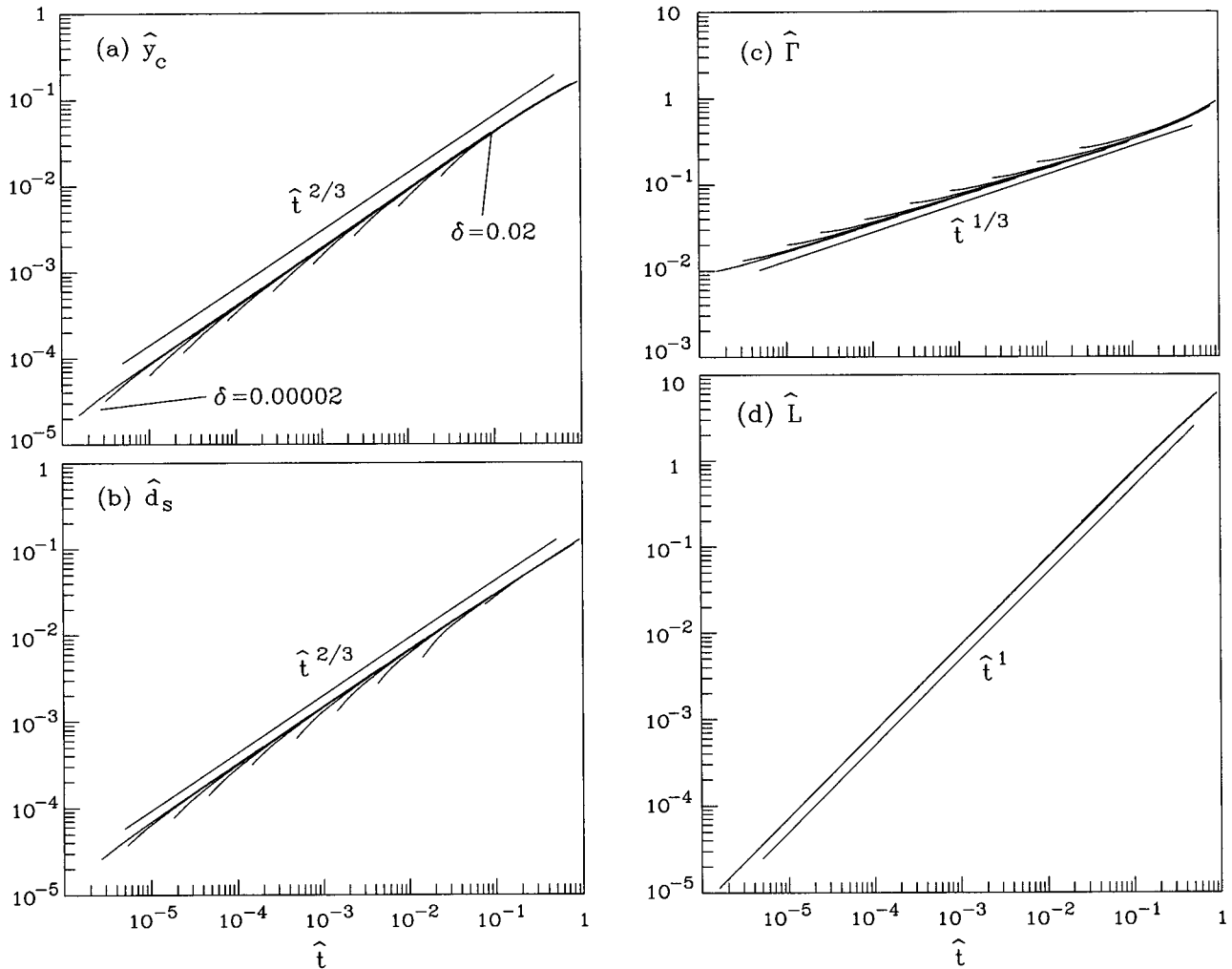
Monika Nitsche

FIG. 5. Log-log plots, for values of $\delta \in [0.00002, 0.02]$ and $m=0$, vs $\hat{t}$. (a) $\hat{y}_c$, (b) $\hat{d}_s$, (c) $\hat{\Gamma}$, (d) $\hat{L}$.

$\hat{L}(\hat{t})$ shown in (d), but the slope $p_L = 1$ appears to fit the data well. The computations for $m = 1/2, 1, 2$ are not shown but the behavior is qualitatively the same as the case $m = 0$ shown here, with the curves differing by a vertical shift. This indicates that the exponents p_q are independent of m but the constants C_q depend on m.
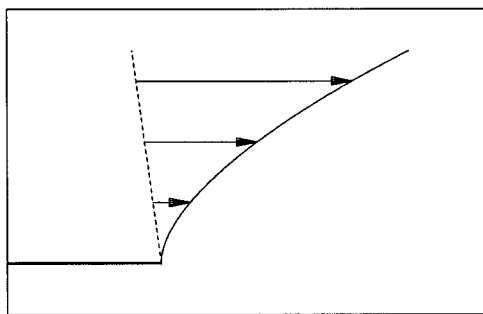

FIG. 6. Computed vortex ring trajectory (solid curve) and extension of the initial upstream trajectory (dashed line). The arrows denote the departure from the initial trajectory. The horizontal line denotes the edge of the tube.

To quantify the power law behavior observed in Fig. 5, we find the values p_q and C_q which best approximate the data in a least squares sense. The least squares approximation is performed over the interval $\hat{t} \in [0.000005, 0.5]$, which is the same interval over which the lines in Fig. 5 are drawn. The results for $m = 0, 1/2, 1, 2$ are shown in Table I. Columns 2–5 in Table I record the powers p_q, columns 6–9 record the constants C_q for the indicated quantities q. The values in parentheses are the values computed by Pullin[2] for the planar separation at the edge of a flat plate. They were inferred from his Figs. 8–9 (for d_s) and Figs. 11–13 (for J and $\omega = \rho_\nu e^{i\chi_\nu}$). Note that Table I describes the behavior of non-dimensional variables as a function of the piston stroke $\hat{t}$. The behavior of the dimensional variables in time t can be recovered from (4) and (5) and the definition of $\bar{U}_o$.

The computed powers p_{y_c}, p_{d_s} and p_Γ in Table I agree well with the similarity theory predictions of 2/3, 2/3 and 1/3, respectively. The constants C_q agree well with the values for planar separation computed by Pullin. The constants C_{y_c} for small m and the constants d_s are within 10%, the constants C_Γ are within 2% of Pullin's computed planar values. As m increases, C_{y_c} increasingly differs from Pullin's
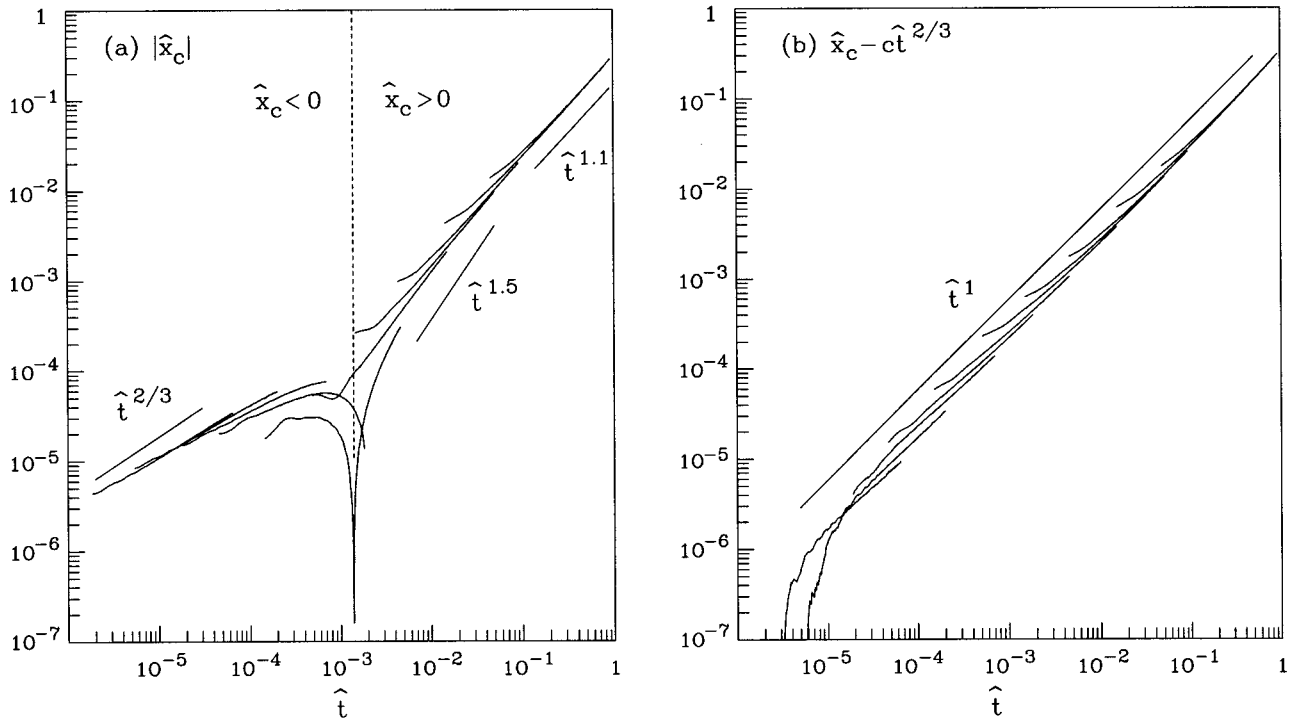
FIG. 7. Log-log plots vs $\hat{t}$ ($m=0$). (a) $|\hat{x}_c|$, (b) $\hat{\alpha}=\hat{x}_c-C_{x_c}\hat{t}^{2/3}$, where C_{x_c} is estimated from the small time behavior in (a).

values. This is attributed mainly to the fact that with increasing m the flow becomes harder to compute.

The values recorded in Table I show that y_c, d_s and Γ in the axisymmetric flow are quantitatively well described by the self-similar planar flow. This is true up to times when the piston stroke is half the tube diameter, even though at these times the ring has travelled downstream and the flow does not resemble the self-similar flow.

The front of the volume of fluid exiting the tube satisfies

$$\hat{L}\approx0.75\hat{t}, \tag{7}$$

for all values of m presented. Equivalently, it travels with approximately 75% of the piston velocity. Since the front is fairly flat, this implies that approximately 25% of the column of fluid leaving the tube opening is displaced and entrained by the vortex ring. To my knowledge there are no experimental records of this behavior of L. A theoretical explanation for the behavior remains to be found.

B. Axial coordinate x_c

Figure 6 shows an envelope of the computed vortex ring trajectory. Almost immediately after leaving the edge of the tube the ring travels downstream (with positive axial veloc-

ity). However, the computations show that the ring first travels upstream (with negative axial velocity) for a short time. The axial coordinate x_c is therefore negative at these initial small times, and positive at later times. Figure 7(a) shows a log-log plot of the absolute value $|\hat{x}_c|$ vs $\hat{t}$, computed with $m=0$ and various values of $\delta \in [0.00002,0.02]$. The figure shows clearly that the ring first travels upstream within the time-interval marked by $\hat{x}_c<0$. This time-interval is small. The piston stroke at which the ring crosses the tube exit plane after its initial upstream motion, indicated by the dashed vertical line, is $\hat{t}_o\approx0.001$.

Figure 7(a) also shows several lines with indicated slopes. The initial upstream motion is seen to satisfy $\hat{x}_c\sim\hat{t}^{2/3}$, as predicted by similarity theory. The large time downstream motion appears to approach linear behavior in the piston stroke. Note that in the transition from $\hat{x}_c\approx0$ to the large time linear behavior, the ring may appear to satisfy $\hat{x}_c\sim\hat{t}^p$ for various p, depending on what time-interval is considered. This may partially explain the differing experimental results observed. Didden[5] quotes a rough estimate of $p=1.5$, Weigand and Gharib[9] observe $p\approx1.1$. One also needs to consider that in these experiments the piston under-

TABLE I. Exponents p_q and constants C_q for the indicated variables $\hat{q}=C_q\hat{t}^{p_q}$. The values computed by Pullin[2] for self-similar planar flow around a flat plate are given in parentheses.

m	p_{y_c}	p_{d_s}	p_Γ	p_L	C_{y_c}	C_{d_s}	C_Γ	C_L
0	0.673	0.658	0.327	1.003	0.199 (0.18)	0.138 (0.15)	0.70 (0.70)	0.756
1/2	0.679	0.658	0.324	1.001	0.178 (0.16)	0.121	0.93 (0.93)	0.739
1	0.684	0.661	0.321	1.004	0.172 (0.14)	0.116 (0.13)	1.16 (1.17)	0.732
2	0.686	0.659	0.320	1.007	0.165 (0.13)	0.111	1.63 (1.67)	0.736

TABLE II. Estimates for the axial coordinate $\hat{x}_c = -C_{x_c}\hat{t}^{2/3} + C_\alpha \hat{t}^{p_\alpha}$. The values computed by Pullin for the self-similar planar flow are given in parentheses.

m	C_{x_c}	C_α	p_α
0	0.027 (0.041)	0.34	1.07
1/2	0.038 (0.061)	0.25	1.05
1	0.040 (0.064)	0.22	1.06
2	0.041 (0.070)	0.19	1.07

goes an initial start-up period and does not satisfy $U_p \sim t^m$ over the time interval studied.

The initial upstream self-similar behavior observed in Fig. 7(a) is indicated by the dashed line in Fig. 6. The arrows in Fig. 6 denote the difference between the observed trajectory and the initial upstream trajectory. This difference $\hat{\alpha} = \hat{x}_c - C_{x_c}\hat{t}^{2/3}$ is plotted in Fig. 7(b), vs $\hat{t}$. The value for C_{x_c} used here is a rough estimate obtained from Fig. 7(a) and is recorded in Table II. The log-log curves in Fig. 7(b) are almost linear, suggesting that $\hat{\alpha}$ also satisfies a power law, $\hat{\alpha} = C_\alpha \hat{t}^{p_\alpha}$. A least squares approximation of the envelope, defined as the minimum over all values of δ, gives estimates for C_α and p_α. The values for p_α recorded in Table II suggest that the downstream component $\hat{\alpha}$ is linear in the piston stroke and

$$\hat{x}_c \approx -C_{x_c}\hat{t}^{2/3} + C_\alpha \hat{t}. \tag{8}$$

This may be understood as follows. Graham[10] noted that near the edge, potential flow out of an opening generally has, to first order, a singular component given by (1) and to second order, a regular component. The potential may be written as $\phi(z) = -c_1 z^{1/2} + c_2 z$, where $z = re^{i\theta}$. The first term in (8) is induced by the singular component of the potential. The second term in (8), the downstream component $\hat{\alpha}$, is induced both by the regular component of the potential as well as by the self-induced vortex ring velocity. These two factors are not present in self-similar planar vortex sheet separation. The similarity theory therefore does not account for the behavior of $\hat{\alpha}$. An explanation for the linear behavior observed here, $\hat{\alpha} \sim \hat{t}$, remains to be found.

We remark that the upstream ring motion observed in our computations occurs at such small times that in a typical experiment, the flow is most likely dominated by viscous effects during these times. It has however been observed in experiments that the ring does not leave the exit plane at the edge of the tube but at a slightly larger diameter[5,9].

C. Shape of the roll-up

The values C_{x_c}, C_{y_c}, C_α, p_α recorded in Tables I and II imply that the piston stroke $\hat{t}_o$ at which the ring leaves the exit plane and the ring diameter at this time increase with m. The values also imply that the upward angle at which the ring leaves the edge decreases with increasing m. This can be observed in Fig. 8a, which shows the computed vortex sheet for $m = 0, 1/2, 1, 2$ at a small time during which the ring
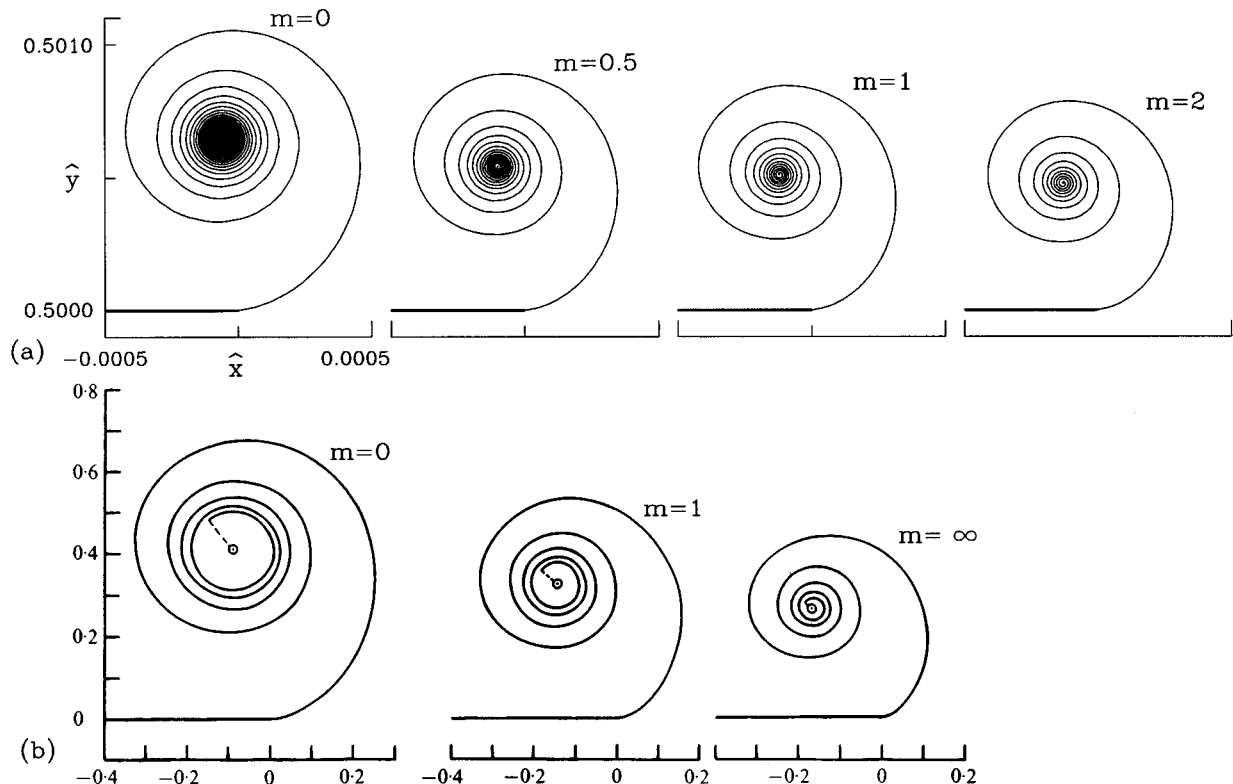

FIG. 8. (a) Computed solution at $\hat{t} = 0.0002$, with $\delta = 0.00004$ and the indicated values of m. (b) Pullin's solution for the self-similar planar roll-up at the edge of a plate (reproduced from Pullin[2]).
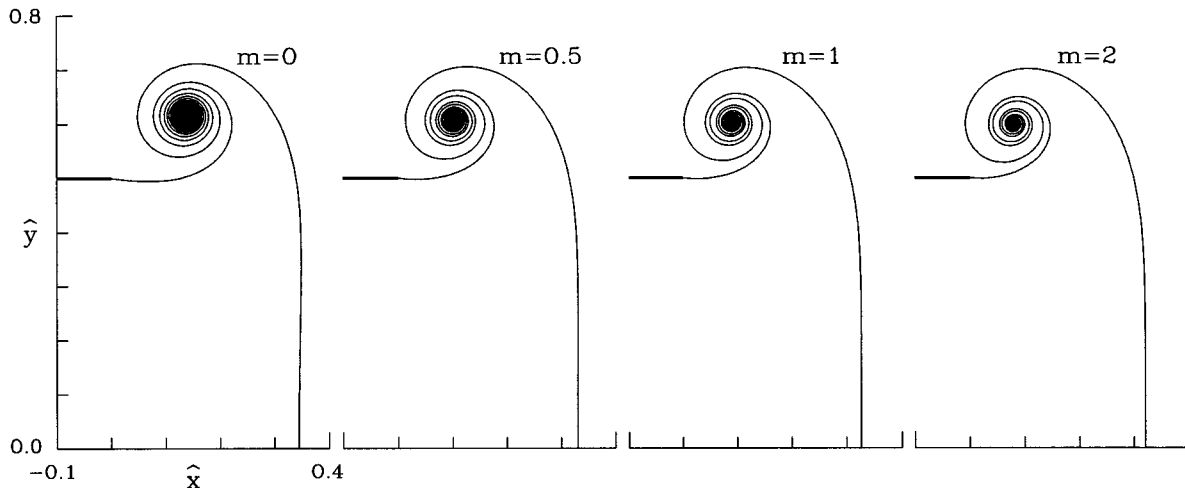
FIG. 9. Computed solution at $\hat{t}=0.5$, with $\delta=0.01$ and the indicated values of m.

is still travelling upstream. For comparison, Fig. 8(b) shows Pullin's[2] solution for the self-similar planar roll-up at the edge of a flat plate, with $m=0,1,\infty$. The outer spiral turns in Figs. 8(a) and 8(b) are in good agreement. In both cases the ellipticity of the roll-up increases with m, the size of the roll-up decreases, and the angle at which the vortex leaves the edge decreases. This angle is larger in Fig. 8(a) than in Fig. 8(b). This is related to the differences in C_{x_c} between the present computations and Pullin's values recorded in Table II. These differences are attributed mainly to the fact that at the initial times considered in Fig. 7, even though they are small, the axisymmetric ring has already departed from self-similar flow.

Some of the features observed in Fig. 8(a) are also observed at large times, when the ring has travelled downstream. Figure 9 shows the solution for piston stroke $\hat{t}=0.5$, near the end of the time-interval described by the scaling behavior observed in Figs. 5 and 7. The material curve which initially lies across the opening is also shown. Both the ellipticity of the roll-up and its tilt with respect to the horizontal increase with m. The front of the fluid volume exiting the tube changes little with m, although one already observes a small departure from (7). The size of the roll-up decreases with increasing m. At the same time, the distribution of outer and inner fluid entrained in the roll-up becomes more asymmetric. For larger m, more of the entrained fluid consists of fluid originally inside the tube, and less of fluid originally outside the tube.

V. SUMMARY

A vortex sheet model was applied to simulate axisymmetric vortex ring formation at the edge of a circular tube. We investigated the dependence of the ring trajectory, circulation, size and shape on the piston velocity, for accelerating velocities $U_p \sim t^m$ and $m=0,1/2,1,2$. The results are compared with theoretical predictions for self-similar planar vortex sheet separation at the edge of a flat plate. The computed behavior is recorded as a function of the piston stroke $\hat{t}$. We

find that for piston strokes up to half the tube diameter and for all values of m considered, the axisymmetric flow is characterized as follows.

(1) The radial ring coordinate y_c, the core size d_s and the circulation Γ are well described by the self-similar planar flow around a flat plate. Appropriately nondimensionalized, they obey the predicted scaling behavior $\hat{y}_c$, $\hat{d}_s \sim \hat{t}^{2/3}, \hat{\Gamma} \sim \hat{t}^{1/3}$. Furthermore, they agree quantitatively with the planar values computed by Pullin. The agreement holds even after the ring has travelled downstream and the axisymmetric flow no longer resembles the planar self-similar flow.

(2) The front of the fluid exiting the tube travels with approximately 75% of the piston velocity, $\hat{L}=0.75\hat{t}$. This behavior has not been previously reported.

(3) The axial coordinate x_c is a superposition of an upstream component predicted by similarity theory and a downstream component which is linear in the piston stroke, $\hat{x}_c = -C_{x_c}\hat{t}^{2/3} + C_a\hat{t}$. As mentioned in the Introduction, Didden[5] observed a discrepancy between experimental measurements and similarity theory predictions for the axial vortex ring coordinate. The present results show that the axial coordinate does satisfy the similarity predictions at very small times but is soon dominated by a downstream component not present in the theory. The downstream component is induced by the ring's self-induced velocity and the regular component of the starting potential flow.

(4) The shape of the rolled-up vortex sheet changes with m. As m increases it becomes more elliptical and decreases in size. The distribution of fluid entrained by the ring becomes more asymmetric. For larger values of m, a larger portion of the entrained fluid consists of fluid initially inside the tube.

ACKNOWLEDGMENTS

bership at the Institute for Mathematics and its Applications. The computations were performed at the IMA.

[1] K. Shariff and A. Leonard, ''Vortex rings,'' Annu. Rev. Fluid Mech. **24**, 235 (1992).

[2] D. I. Pullin, ''The large-scale structure of unsteady self-similar rolled-up vortex sheets,'' J. Fluid Mech. **88**, 401 (1978).

[3] P. G. Saffman, ''The number of waves on unstable vortex rings,'' J. Fluid Mech. **84**, 625 (1978).

[4] D. I. Pullin, ''Vortex ring formation at tube and orifice openings,'' Phys. Fluids **22**, 401 (1979).

[5] N. Didden, ''On the formation of vortex rings: Rolling-up and production of circulation,'' J. Appl. Math. Phys. (Z. Angew. Math. Phys.) **30**, 101 (1979).

[6] M. Nitsche and R. Krasny, ''A numerical study of vortex ring formation at the edge of a circular tube,'' J. Fluid Mech. **276**, 139 (1994).

[7] R. Krasny, ''Vortex sheet computations: Roll-up, wakes, separation,'' Lect. Appl. Math. **28**, 385 (1991).

[8] L. Prandtl and O. G. Tietjens, *Fundamentals of Hydro- and Aeromechanics* (McGraw-Hill, New York, 1934), Sec. 93.

[9] A. Weigand and M. Gharib, ''On the evolution of laminar vortex rings'' (preprint).

[10] J. M. R. Graham, ''Vortex shedding from sharp edges,'' Imperial College Aero Report No. 77-06, ISSN 03087247, 1977.

Phys. Fluids, Vol. 8, No. 7, July 1996

Monika Nitsche   1855